# Microwave spectroscopy of two-photon transitions in connection with a double Stark resonance in sodium Rydberg atoms

I. M. Beterov, A. O. Vyrodov, I. I. Ryabtsev, and N. V. Fateev

*Institute of Semiconductor Physics, Siberian Branch of the Russian Academy of Sciences*

The two-photon absorption and double resonance on the $nP \to (n + 1)P$ microwave transitions of Na Rydberg atoms have been studied experimentally in a static electric field (the double Stark resonance). The static polarizabilities of the $nP$ states with $n = 36$ and 37 have been measured in weak electric fields. Deviations from the quadratic Stark effect due to avoided crossings have been observed. The conditions for the occurrence of a double Stark resonance due to a crossing of a real intermediate level and a virtual level of a two-photon transition have been studied as functions of the microwave frequency and the electric field. The critical frequencies and fields are calculated. It is demonstrated that the double Stark resonance can be utilized for an absolute calibration of electric fields in vacuum. "High-field" effects have been observed.

## 1. INTRODUCTION

Two-photon transitions and double resonances in quantum systems have attracted research interest for many years now (Ref. 1, for example). These physical effects, which are observed in intense optical, ir, and rf fields, underlie methods of nonlinear spectroscopy.[2–5] Two-photon spectroscopy, the double optical resonance, the ir-microwave resonance, etc., are used to study electronic transitions, vibrational-rotational transitions, purely rotational transitions, and the magnetic structure of atoms, molecules, and ions in the gas phase as well as in condensed media.

Underlying both methods is the theory of the interaction of monochromatic or bichromatic coherent light with a three-level quantum system, limited in the simplest case to second-order perturbation theory.[6–8] The two-photon process includes the concept of a virtual state. Consequently, the relative contributions of two-photon and two-step (cascade) transitions near or exactly at a resonance in terms of an intermediate state remained a key question for a long time. This question was examined in detail in Refs. 8 and 9. It was demonstrated experimentally in Ref. 10 that the cross section for two-photon absorption on the $3S$–$5S$ transition of Na increases toward the resonance with the intermediate $3P$ state. This point was demonstrated by simultaneously varying the frequencies of two lasers in such a way that the sum of these frequencies remained constant, at the value corresponding to the two-photon resonance. In observations of two-photon transitions between low-lying states in atoms and also molecules, it is essentially impossible to cause any substantial change in the energy defect between the virtual level through which the two-photon transition goes and the real intermediate state which is responsible for the double resonance if the frequency of the electromagnetic field is fixed.

A different situation becomes possible when Rydberg (highly excited) states of alkali metal atoms are used. Because of the particular values of the quantum defects of the $S$ and $P$ states of these atoms at main quantum numbers $n > 20$, there is a system of nearly equidistant levels (Fig. 1a). Two-photon $nP \to (n + 1)P$ transitions occur in a three-level scheme with a nearly resonant intermediate level. Figure 1b shows the detuning of the real $S$ level from the virtual level for the two-photon $nP \to (n + 1)P$ transition when the principal quantum number $n$ changes.

It can be shown that the imposition of a weak electric field, for which the quadratic-Stark-effect approximation is still valid, leads to crossing of a virtual state and a real intermediate state. It also leads to the occurrence of the $nP \to (n + 1)S \to (n + 1)P$ double resonance. Both the critical electric field and the frequencies of the microwave field are fixed.

Since the dipole moments for transitions between neighboring $S$–$P$ states of Rydberg atoms in the microwave range are huge, it is a simple matter to achieve values of the saturation parameter well above one and to study the characteristics of double resonances in strong and ultrastrong resonant fields, as functions of frequency and the static electric field. The fine structure of $nP$ states of alkali metal atoms may lead to additional structural features in the double Stark resonance as the result of interactions between quantum transitions and their mutual interference.

In this paper we are reporting an experimental study of two-photon absorption and a double resonance on microwave transitions of Na Rydberg atoms (a double Stark resonance). We have studied the conditions for the occurrence of the double Stark resonance and the features of this resonance as functions of both the microwave frequency and the electric field. We have measured the static polarizabilities of the $P$ states. We have found deviations from the quadratic Stark effect and the dependence of the polarizabilities on the projection of the total angular momentum $J$. We have calculated critical frequencies and evaluated the possibility of using the double Stark resonance for an absolute calibration of electric fields in vacuum. We have observed "high-field" effects.

## 2. EXPERIMENTAL APPARATUS AND PROCEDURE

The Na Rydberg atoms were produced in $nP$ ($n = 36$ and 37) states in an atomic beam. For this purpose, we used the three-step scheme $3S_{1/2} \to 3P_{3/2} \to 4S_{1/2} \to nP_{1/2,3/2}$, synchronized by the output pulses from two dye lasers, with wavelengths $\lambda_1 = 589$ nm and $\lambda_2 = 680$–$630$ nm (in the first and third steps), and also by the output pulses from a
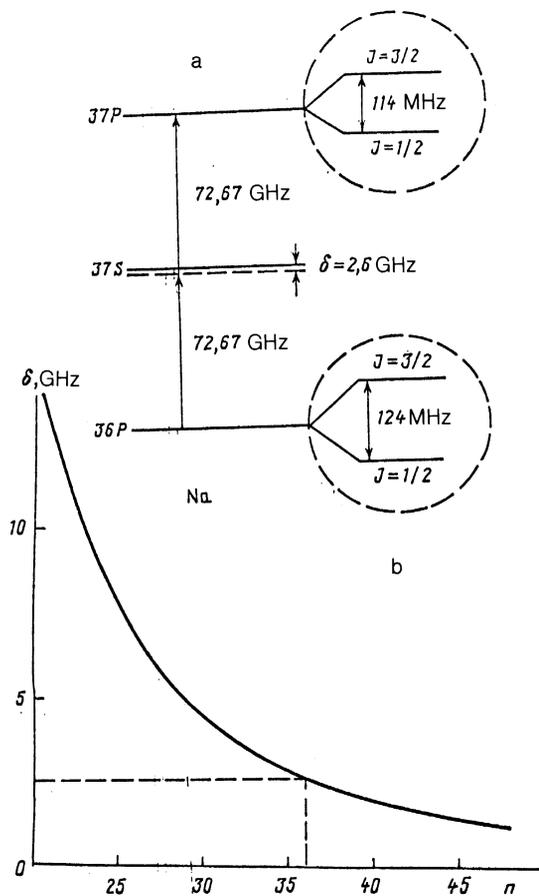
FIG. 1. a—Scheme of two-photon $nP \to (n + 1) P$ transitions in Na Rydberg atoms with allowance for the fine structure; b—detuning of the real intermediate $(n + 1)S$ level and the virtual level of the two-photon transition along the frequency scale versus the main quantum number $n$.



FIG. 2. Experimental layout for millimeter-wave spectroscopy of two-photon transitions in Na Rydberg atoms. a: General layout. 1—Source of the atomic beam; 2—plates of a copper capacitor; 3—VÉU-6 channel electron multiplier; 4—laser beam; 5—atomic beam; 6—waveguide microwave-radiation input. b: Schematic diagram of the optical and electrical apparatus. 1-3—Tunable lasers for optical excitation; 4-6 and 12—trigger generators and sync units; 7-9—pulse shapers; 10—tunable backward-wave-tube source of millimeter-wave radiation; 11—cathode follower; 13—frequency meter; 14—analog-to-digital converter; 15—chart recorder; 16—pulse counter with electronic switch; 17—oscilloscope.

laser using $F_2^-$ color centers in a LiF crystal, operating at a wavelength $\lambda_2 = 1.14$ mk, in resonance with the $3P_{3/2} \to 4S_{1/2}$ transition. For pumping we used the output from an Nd:YAG laser ($\lambda = 1.06 \mu m$), its second harmonic ($\lambda = 532$ nm), and the beam from a copper-vapor laser ($\lambda = 510.8$ nm). All the lasers were operated at a high pulse repetition rate ($\sim 10$ kHz). The pulse length was in the range 20–100 ns. The optical layouts of the lasers and their characteristics are described in more detail in Refs. 1 and 12.

The beams from the three lasers were brought into coincidence by dichroic mirrors and were coupled into a vacuum chamber, in which a warm beam of Na atoms was excited into Rydberg states (Fig. 2). These light components were focused by means of a quartz lens with a focal length of 30 cm (the caustic size was $\sim 200 \mu m$). This focusing raised the laser power density in the interaction region, while allowing us to avoid surface-ionization effects at the metal walls. We achieved saturation in the first and second steps. In the third step, because of the decrease (as $n^{-3}$) in the probability for a dipole transition,[13] we were not able to achieve saturation in the $n = 36$ case. The fluctuations in the number of Rydberg atoms from pulse to pulse were thus determined primarily by fluctuations in the laser power and frequency in the third
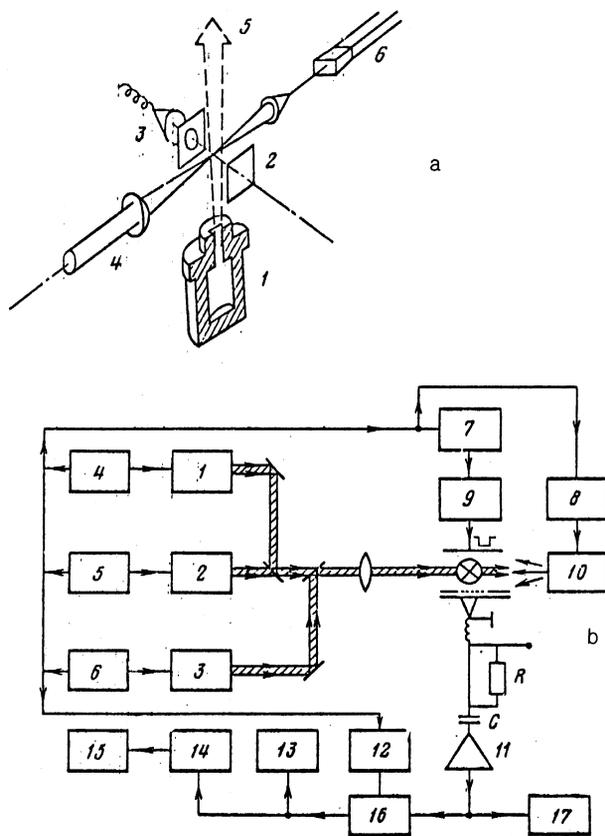
step. The ultimate excitation efficiency was $\sim 10^{-4}$. At a number density $\sim 10^7$ cm$^3$ of the atoms in the beam, and at the interaction volume $\sim 10^{-3}$ cm$^3$, there were accordingly one or two Rydberg atoms per pulse.

The atomic beam was produced through an effusion of Na vapor from the slit ($0.5 \times 3$ mm$^2$) of a source heated with a tungsten filament. The source temperature was measured by a calibrated Chromel–Alumel thermocouple. The source temperature $T$ was held constant to within 0.5 °C by means of an automatic temperature regulator. Under the experimental conditions, the number density of atoms in the interaction zone was varied over the range $10^7$–$10^8$ cm$^{-3}$. The arithmetic velocity of the bulk of the sodium atoms in the beam was $v_{max} = (2kT/M)^{1/2}$, where $M$ is the mass of the sodium atom. These are the atoms which one would expect to dominate the signal, because of the long lifetimes of Na Rydberg atoms with $n > 20$ (Ref. 11, for example). The typical source temperature in the experiments was $T = 513$ K. This figure corresponds to $v_{max} = 6 \cdot 10^4$ cm/s. The atoms moved a distance $\sim 10 \mu m$ during the excitation pulse

($\tau \sim 20$ ns), so these atoms could be regarded as immobile during the excitation process, and the excitation region could be regarded as localized in the caustic of the laser beam.

A diaphragm 4 cm away from the source slit served as a collimator of the atomic beam, determining the divergence of this beam ($\lesssim 10^{-2}$ rad). A differential pumping system was used. The residual pressure in the chamber was $10^{-6}$–$10^{-7}$ torr and was determined by gas evolved from the heated beam source. The atoms were excited into Rydberg states in an interaction volume 13 cm away from the slit of the beam source. This interaction volume was a plane capacitor with copper plates 33 mm in diameter, separated by a distance of 7.5 mm. One of the plates was grounded and had an aperture 10 mm in diameter, covered by a grid. The aperture was for the extraction of charged particles. A negative electric pulse, generated by a high-voltage pulse amplifier, was applied to the second plate of the capacitor.

The signal from a vacuum-tube square-pulse generator was fed to the amplifier input. This generator was triggered by a master oscillator with a continuously adjustable delay. A high-voltage signal of square shape with a length of 2 $\mu$s and an adjustable height was generated at the output of the pulse amplifier. The maximum field between the capacitor plates was $\sim 2$ kV/cm. There was also provision for applying a static electric field up to 1 kV/cm. This static field made it possible to bring the pulses of the first and second steps into coincidence in terms of the signal representing the three-photon ionization of Na. The use of a strong pulsed electric field made it possible to effectively detect highly excited atoms by the method of selective field ionization.[14] The characteristics of the pulse were such that the field ionization was adiabatic.[15]

Photoelectrons were detected by means of a VÉU-6 channel multiplier with a gain of $10^8$ and a thermal background of 0.5 pulse/s. The one-electron pulses from the VÉU-6 had a Poisson pulse-height distribution and an average pulse height of 300 mV.

The electrical signal from the electron multiplier was fed through an amplifier to the inputs of an oscilloscope and to a pulse counter with a pulse-height discriminator and a controllable switch. This approach made it possible to detect pulses at a certain time, specified by an external generator synchronized with the pulses from the pump laser. We measured the number of pulses at the output of the electron multiplier with a buildup time of 1 s at a repetition frequency $\sim 10$ kHz. The counting of the pulses was kept linear through the appropriate choice of the frequency of the pulses in the signal of interest: $f_s \ll f_L$, where $f_L$ is the repetition frequency of the laser excitation pulses. In the linear regime, $f_s$ is proportional to the number of atoms which are ionized by the electric field in the detection zone. By working in the pulse counting regime we were able to avoid problems which would arise from the scatter in the amplitudes of the one-electron signals from the VÉU-6.

In addition to the field-ionization signal, which appeared at the instant the electric field pulse was applied, we detected a signal representing the three-step photoionization of Na atoms from the $4S_{1/2}$ state by the laser of the first step during the application of the laser excitation pulses. This signal was convenient for use in adjusting the laser wavelengths, but when this signal was fed to the counter is was

necessary to distinguish the time-delayed field-ionization signal by means of an auxiliary strobe pulse.

In experiments on the microwave spectroscopy of transitions between Rydberg atoms, including transitions which occur in a static electric field, the high sensitivity of Rydberg atoms to the weak residual electric fields and the thermal radiation is an important factor. Accordingly, in several of the experiments we departed from the procedure of Refs. 11 and 12 and used a modified two-chamber system, which made it possible to spatially separate the regions of excitation, of interaction with the microwave field, and of detection by means of field ionization. This system consisted of two plane copper capacitors with plates separated by a distance of 8.4 mm. Each of the capacitors was fitted with a VÉU-6 channel multiplier to detect the highly excited Rydberg atoms which passed through the capacitors in succession. This approach made it possible (for example) to excite Rydberg atoms near the first electron multiplier, where there was no electric field for the detection of these atoms, and it was possible to carry out a spectroscopy of microwave transitions, and then to detect the population of these atoms in the second chamber. The first electron multiplier was used to monitor the density of Rydberg atoms in the excitation and interaction region. Careful shielding of both capacitors with a copper shield reduced the level and variations in the residual electric fields in the regions of excitation, interaction, and detection to values $< 5$ mV/cm. These residual fields could be monitored by a Stark-spectroscopy technique developed especially for the purpose, with the help of a waveguide $CO_2$ laser.[16] Alternatively, these fields could be determined from the broadening of the microwave resonances.

In order to eliminate effects stemming from the thermal radiation from the walls of the working chamber and the beam source, the copper capacitors, the shields, the diaphragms, and the electron multiplier were all cooled to liquid-nitrogen temperature (77 K). This cooling sharply reduced the noise associated with the photoionization of Rydberg atoms by thermal radiation and collisional ionization.[11,12] It also increased the density in the detection region by virtue of an increase in the lifetime. The transit time taken by a Rydberg atom to move from the interaction region to the detection region was 50 $\mu$s. This time was comparable to the lifetime of a Rydberg atom in a state with $n \approx 30$.

The copper shield near the first electron multiplier was constructed in such a way that the open end of the rectangular waveguide could be inserted into the interaction zone, while the beam from the $CO_2$ laser could be fed in through an additional NaCl window. There was also provision for laser excitation of Rydberg atoms at two different points in the warm beam. One point was opposite the entrance aperture of the first electron multiplier; the second was 1 cm downstream along the flux. It was thus possible to study transit-time effects. The elimination of the thermal radiation also made it possible to reduce the rate at which Rydberg states with different angular momenta mixed and to record spectra with a high signal-to-noise ratio.

In the experiments we use the tunable monochromatic output from a backward-wave generator in the range 53.57–78.33 GHz ($\lambda$ accordingly varied from 5.6 mm to 3.8 mm). The width of the line was $\lesssim 3$ MHz.

The generator power at the entrance to the waveguide could be varied up to 30 mW; it was measured with a ther-

mistor detector. The microwave power in the region of the interaction with the atoms was estimated crudely under the assumption of a point radiator without losses at the end of the waveguide. A more precise calibration was carried out using the dynamic Stark effect[17] and the field-induced broadening of two-photon resonances.

In order to eliminate the noise associated with laser power fluctuations in the third excitation step and fluctuations in the number of excited atoms in the interaction zone, we developed a novel detection system, in which the signal depended only weakly on these parameters. As before, the analysis was carried out in a pulse counting mode, so that the measurements would be carried out in a linear regime. Figure 3 shows time diagrams of the excitation and detection pulses.

As a time 0.7 $\mu$s after the end of the laser pulse (Fig. 3a), the microwave field pulse was applied (Fig. 3b), with a frequency close to the frequency of the transition under study (which we will call the $1 \rightarrow 2$ transition). This 0.7-$\mu$s delay was necessary in order to separate the laser pulse which excited level 1 from the microwave pulse. In this case the $1 \rightarrow 2$ transition could be regarded as isolated. The microwave field interacted with the Rydberg atoms for 2.5 $\mu$s. This time was long enough that some of the atoms could go from the lower excited state, 1, into the higher excited state, 2. States 1 and 2 have different critical fields for selective field ionization ($E_{cr}^{FI} \propto 1/n_{eff}^4$). By applying a two-step pulse (Fig. 3c) to the plates of the plane capacitor in the detection system, we can select the heights of the steps in such a way that the first step ionizes only the atoms in state 2, while the second step ionizes the atoms which remain in state 1. There



was also provision for adding a weak static field to this pulse in order to study the Stark effect on microwave transitions.

It was thus possible to analyze the signals from levels 1 and 2 independently (Fig. 3d), distinguishing them by means of strobe pulses (Fig. 3e) and then measuring the frequencies at which the pulses for each signal appear. We are interested in the population of level 2, since it is determined by the probability for the $1 \rightarrow 2$ transition. In the pulse counting mode the signal from level 2 is proportional to the number of atoms detected in level 2 after a certain specified measurement time $T_m$:

$$S = CN_2(T_m),\qquad(1)$$

where the coefficient $C$ determines the probability for electron detection by the VÉU-6. Here the transit time in the detection zone is taken into account. This coefficient depends on the temperature of the atomic beam and the size of the entrance window of the VÉU-6. It is a constant for signals from all levels, provided that their lifetime is substantially longer than the transit time through the detection zone. The measurement time $T_m$ should be long enough ($T_m \gg f_L^{-1}$, where $f_L$ is the repetition frequency of the laser pulses) to provide an adequate statistical base for the analysis of the signals. In this we can write

$$S = CT_m f_L N_1(t=0) W(1 \rightarrow 2),\qquad(2)$$

where $N_1(t=0)$ is the number of atoms in state 1 which are formed per laser pulse, and $W(1 \rightarrow 2)$ is the probability for the $1 \rightarrow 2$ transition during the application of the microwave pulse.

The measurement time $T_m$ is determined by the instant at which the sum of the number of pulses from atoms in state 2 and the number of pulses from atoms remaining in state 1 reaches a certain specified number $z$. If we ignore the relaxation of levels 1 and 2, we can write

$$z = Cf_L T_m N_1(t=0),\qquad(3)$$

since the total number of atoms in states 1 and 2 is a constant. Expression (3) determines the detection time $T$. Substituting $T$ into (2), we find an expression for the signal in our detection system:

$$S = zW(1 \rightarrow 2).\qquad(4)$$

This signal is sent to a chart recorder with the help of a digital-to-analog converter. The signal in the detection system is thus determined, in a first approximation, exclusively by the probability for the $1 \rightarrow 2$ transition. It is independent of the power levels of the lasers and independent of the density of atoms in the beam. It thus becomes possible to substantially reduce the noise level during the recording of the spectra of microwave transitions between Rydberg states. However, we should stress again that expression (4) was derived by ignoring the relaxation of levels 1 and 2. In a study of transitions near the $36P$ level, this simplification is completely legitimate, since the radiative lifetime ($\approx 164$ $\mu$s) is far longer than the time scale in the recording system (5 $\mu$s), when we allow for the decrease in the lifetime due to the thermal radiation at 77 K.

There is yet another circumstance which complicates the use of expression (4): Our experiments were on levels having fine structure. For the $36P$ level, for example, the
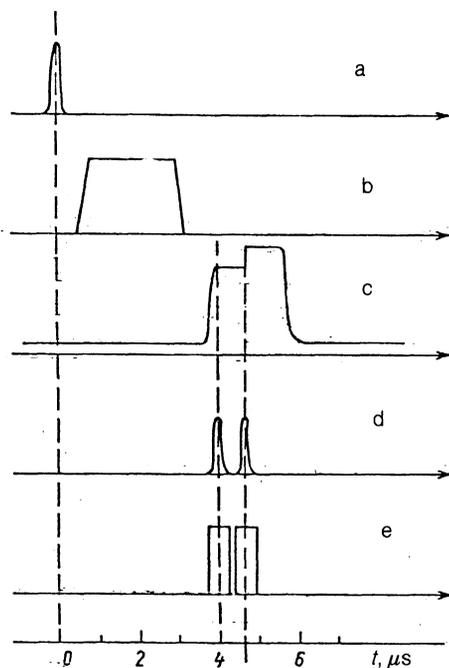
FIG. 3. Time diagram of the excitation and detection pulses. a—Laser pulse; b—microwave field pulse; c—doubled field-ionization pulse; d—electronic pulses representing the densities of atoms in the upper and lower working states; e—strobe pulses in the signal processing.

619     Sov. Phys. JETP **74** (4), April 1992

Beterov *et al.*     619

fine-structure interval between the $J = 1/2$ and $J = 3/2$ components is 124 MHz. The linewidth of the microwave source, on the other hand, is less than 3 MHz, so the $1 \rightarrow 2$ transition occurs between the fine-structure components of these levels. In this situation, only one of the fine-structure sublevels of the lower level is emptied, while the normalization according to (3) is carried out on the basis of the total number of atoms in level 1. Expression (4) should thus be multiplied by the relative population of that fine-structure sublevel of the lower level (1) from which the $1 \rightarrow 2$ transition occurs. The fluctuations in the relative populations of the fine-structure sublevels, however, are not canceled out. Consequently, the signal is given by the following expression for our detection system, in the case of spectroscopy of microwave transitions between fine-structure components of the excited state:

$$S = z \frac{\rho_1(J)}{\sum_J \rho_1(J)} W(1 \rightarrow 2), \qquad (5)$$

where $\rho_1(J)$ is the population of the fine-structure sublevel of level 1. The quantities $\rho_1(J)$ are determined by the probabilities for one-photon transitions from level $4S_{1/2}$ to various sublevels of the fine structure of level 1 and are proportional to the beam intensity of the third-step laser. The signal-to-noise ratio in our microwave-spectroscopy experiments was typically greater than 20; such ratios are completely adequate for obtaining reliable spectra. The detection system could also be operated on line with a computer to process the signal with the help of CAMAC facilities, since the measurements are carried out in a pulse-counting mode. Below we reproduce some of the spectra obtained through the use of the DVK-3 interactive computer complex.

## 3. SPECTROSCOPY OF THE TWO-PHOTON TRANSITION $36P \rightarrow 37P$ Na; FINE STRUCTURE AND FIELD EFFECTS

In the absence of external fields, the spectrum of the $36P \rightarrow 37P$ two-photon transition should have four peaks, corresponding to transitions between the various fine-structure components. The energies of the fine-structure sublevels of the $36P$ and $37P$ levels, as well as those of the intermediate $37S$ level, can be calculated from the values of the quantum defects for the $S$ and $P$ levels, which were measured with high accuracy in Ref. 18. For the level with principal quantum number $n$, these values are

$$\delta(nS_{1/2}) = 1,3479692(4) + \frac{0,06137(10)}{[n - 1,3479692(4)]^2},$$

$$\delta(nP_{1/2}) = 0,855424(6) + \frac{0,1222(2)}{[n - 0,855424(6)]^2}, \qquad (6)$$

$$\delta(nP_{3/2}) = 0,854608(3) + \frac{0,1220(6)}{[n - 0,854608(3)]^2}.$$

The numbers in parentheses are the experimental errors in the last significant figure. The value of the Rydberg constant for the Na atom is[18]

$$R_{\mathrm{Na}} = 3,289763408(20) \cdot 10^{15} \text{ Hz}. \qquad (7)$$

The position of the $37S$ intermediate level, which is almost exactly halfway between the $36P$ and $37P$ levels [the distance between the virtual level of the two-photon transition

and the real $37S$ level is about 2.6 GHz at a transition frequency of 72.6 GHz (Fig. 1)], allows us to treat the $36P \rightarrow 37P$ two-photon transition in the three-level approximation, at least for weak microwave fields.[17]

Figure 4a shows the experimental spectrum of the $36P \rightarrow 37P$ two-photon transition; Fig. 4b shows the corresponding spectrum for the $37P \rightarrow 38P$ transition. We find four components in the spectrum, which correspond to the transitions (in order of increasing frequency)

$$36P_{1/2} \rightarrow 37P_{1/2}, \ 36P_{1/2} \rightarrow 37P_{3/2}, \ 36P_{3/2} \rightarrow 37P_{1/2}, \ 36P_{3/2} \rightarrow 37P_{3/2}.$$

The positions of the two-photons resonances and the frequency intervals between them agree quite accurately (within about 1%) with values calculated from relations (6) and (7), which are shown in Fig. 1. As expected, the transition $36P_{3/2} \rightarrow 37P_{3/2}$ has the highest intensity, and $36P_{1/2} \rightarrow 36P_{1/2}$ the lowest. The primary reason for these results is the difference in the dipole moments of the transitions from these levels to the intermediate $37S$ level.

Repeated recordings of this spectrum have shown that the peak intensities depend on the tuning of the resonator of the third-step laser, because of the change in the rate at which the fine-structure components are excited and also because of the change in the discrimination threshold of the detection system. The reproducibility of the spectrum is quite good. This reproducibility is evidence that the fluctuations in the frequencies of the resonator modes of the third-step laser are averaged out over the measurement time and become inconsequential. Another point to bear in mind is
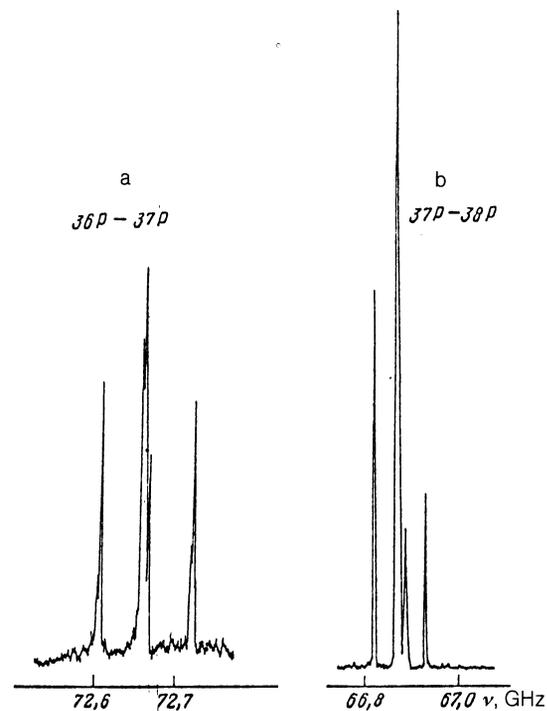


FIG. 4. Microwave spectrum of the two-photon absorption, with resolved fine structure. a—Absorption on the transition $36P \rightarrow 37P$; b—on the transition $37P \rightarrow 38P$. The power density of the microwave field is $> 10^{-6}$ W/cm$^2$.

that the Rydberg atoms travel about 2 mm during their interaction with the microwave field. This distance is close to the wavelength of the microwave radiation, so an atom interacts with some spatial average value of the microwave field. The spatial distribution of the field may vary with the frequency of the microwave radiation, since this radiation is coupled from the open end of the waveguide into the region of the copper plane capacitor, in which standing waves may arise.

The microwave power was calibrated on the basis of the field-induced broadening of the $36P_{1/2} \rightarrow 37P_{3/2}$ transition; the corresponding spectra are shown in Fig. 5. The width of the resonance is determined by the Rabi frequency of the two-photon transition, which was measured in Ref. 17. In the approximation of a three-level scheme, the population of the upper level for the two-photon transition is described by[19]

$$n_2 \sim \frac{|\gamma_{02}|^2}{(\Omega - \Omega_{opt})^2 + |\gamma_{02}^2|}, \tag{8}$$

where $\Omega$ is the microwave frequency (an angular frequency), $\Omega_{opt}$ is the optimum frequency of the two-photon transition, when the shift of the levels due to the dynamic Stark effect is taken into account, and $\gamma_{02}$ is the two-photon Rabi frequency. The latter is given by

$$|\gamma_{02}|^2 = \frac{\varepsilon^2}{4\pi^2\delta} |\langle 36P_J | \mathbf{De} | 37S_{1/2} \rangle \langle 37S_{1/2} | \mathbf{De} | 37P_{J'} \rangle|, \tag{9}$$

where $\varepsilon$ is the microwave field strength, $\delta$ is the distance from the real intermediate $37S$ level to the virtual level for the two-photon transition, and $\mathbf{De} = D_z$ is the projection of the vector dipole moment of the electron onto the wave polarization vector. For the field-induced broadening on a two-photon transition, expression (8) gives us (this is an ordinary frequency now)

$$\Delta v = \frac{\varepsilon^2}{8\pi^2\hbar^2\delta} |\langle 36P_J | D_z | 37S_{1/2} \rangle \langle 37S_{1/2} | D_z | 37P_{J'} \rangle|, \tag{10}$$

if the $z$ axis runs parallel to the wave polarization vector, e. Only the matrix elements for transitions with $\Delta M = 0$ are nonzero in (10). The radial parts of the matrix elements for the $36P \rightarrow 37S$ and $37S \rightarrow 37P$ transitions can be calculated from the formula given in Refs. 20 and 21. The results are $1445ea_0$ and $1487ea_0$, respectively. The angular factors calculated in the approximation of $LS$ coupling from the equations in Ref. 22 are $1/3$ for the transition $36P_{1/2} \rightarrow 37S_{1/2}$ and $2^{1/2}/3$ for the transition $37S_{1/2} \rightarrow 37P_{3/2}$ for $\Delta M = 0$. As a result we find the relationship between the field-induced
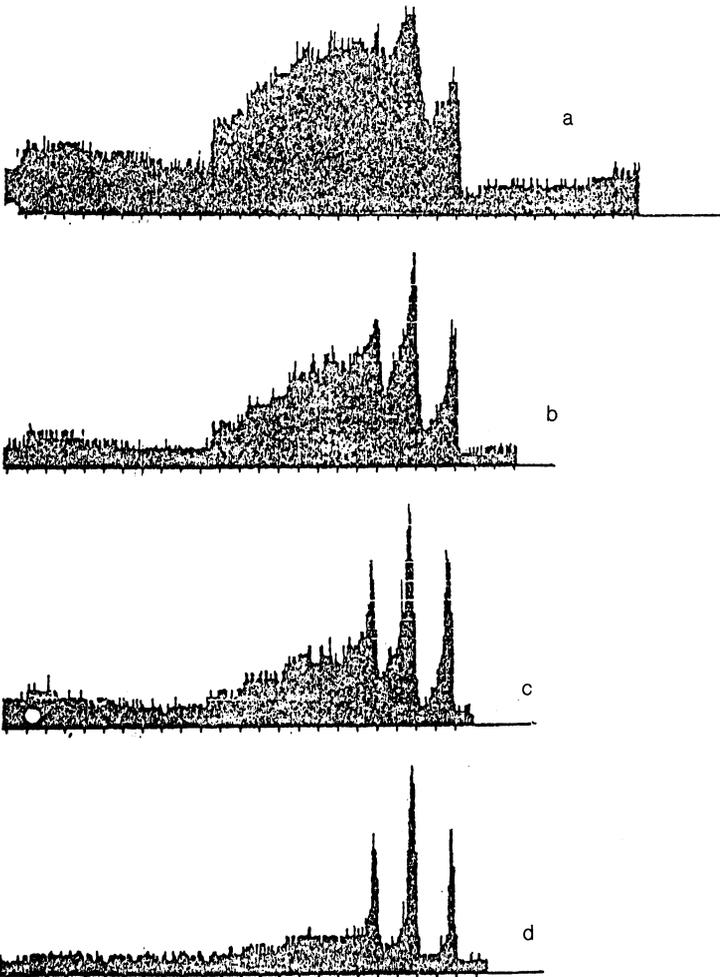


FIG. 5. Field-induced broadening of the spectra of the two-photon absorption on the $36P \rightarrow 37P$ transition for various microwave intensities. a—$10^{-3}$ W/cm²; b—$4 \cdot 10^{-4}$; c—$2.5 \cdot 10^{-4}$; d—$10^{-4}$ W/cm². These recordings were generated in the course of processing in a CAMAC and DVK-3 complex.

broadening of the two-photon transition $36P_{1/2} \to 37P_{3/2}$ and the microwave intensity:

$$\Delta \nu (\text{MHz}) \approx 10^5 I \ (\text{W/cm}^2). \quad (11)$$

The asymmetry of the field-induced broadening of the two-photon resonance is interesting. It apparently stems from a line shift in a spatially nonuniform and intense microwave field. Similar effects have been observed in the optical region in the spectroscopy of the two-photon absorption on the $3s \to 5s$ Na transition.[10] A point which remains unclear is the physical nature of the wide, continuous absorption band at the maximum microwave power. Because of the pronounced nonlinearity of the effect, this band might be linked with the existence of weak standing waves at frequencies different from the frequency of the two-photon resonance.

The observation of strong-field effects in these experiments is a consequence of the huge dipole moments for transitions between neighboring Rydberg states and the small distance between the real intermediate $37S$ level and the virtual level of the two-photon transition $36P \to 37P$. The transition frequencies observed agree well with the experimental results of Ref. 18.

## 4. STATIC STARK EFFECT ON THE TWO-PHOTON TRANSITION 36P→37P; DOUBLE STARK RESONANCE

A static electric field causes a shift and a splitting of the fine-structure components of the $36P$ and $37P$ levels. It also causes a shift of the $37S$ intermediate level. Generally speaking, the total angular momentum $J$ is not conserved in an electric field; only its projection onto the electric field ($M$) is conserved. In sufficiently weak fields, on the other hand, the interaction of an atom with a static external electric field can be described by perturbation theory.[22] In the case of $LS$ coupling, the first nonvanishing term of the perturbation theory is quadratic in the external field $E$. The behavior of the energy levels in a weak electric field is described in general by

$$\Delta E_{JM} = -\frac{1}{2} \left[ \alpha_0 (nl) + \alpha_2 (nlJ) \frac{3M^2 - J(J+1)}{J(2J-1)} \right] E^2, \quad (12)$$

where $\alpha_0 (nl)$ and $\alpha_2 (nlJ)$ are respectively the scalar and tensor polarizabilities of level $nlJM$. The scalar polarizability describes the shift of the center of gravity of the fine-structure component, while the tensor polarizability describes its splitting in the electric field. The component $J = 1/2$ does not split, because of the relation $\alpha_2 \sim (2J-1)^{1/2}$, and the fraction in (12) becomes unity. The $nl$ dependence of $\alpha_0$ and $\alpha_2$ can be described by

$$\alpha_{0,2} = C_{0,2} (n_{\text{eff}})^7, \quad (13)$$

where $n_{\text{eff}}$ is the effective principal quantum number of level $nl$, and the constants $C_{0,2}$ depend weakly on $n_{\text{eff}}$ (Ref. 23).

Expression (12) is valid only as long as the shift of the given level in the electric field is smaller than the distance to the nearest neighboring level. When this condition is violated, energy levels of different parities mix, and we can no longer use perturbation theory. In sufficiently strong fields, the quadratic Stark effect becomes the linear effect characteristic of the hydrogen atom, but (in contrast with hydrogen-atom case) the energy levels in atoms of alkali metals do

not cross in the electric field (this is an "anticrossing" effect[20]).

The Stark effect on the two-photon transition $36P \to 37P$ was studied in weak fields ($< 10$ V/cm). As a result, the behavior of the energy levels in the electric field was approximately quadratic. Figure 6 shows the Stark diagram of the $36P$, $37P$, and $37S$ levels (this figure is not drawn to scale in terms of frequencies).

The electric field lifts the degeneracy with respect to the absolute value of the angular-momentum projection $|M|$, but the twofold degeneracy of each of the Starks of levels $J$, $|M|$ with respect to the direction of the projection of the angular momentum remains. In an electric field, this spectrum of the two-photon transition $36P \to 37P$ should have nine components, corresponding to transitions between the various Stark sublevels.

Figure 7 shows experimental spectra of the two-photon transition $36P \to 37P$ (a) in the absence of an electric field and (b) in a weak electric field, of 2.2 V/cm. The microwave power was chosen in such a way that the heights of the signals in the Stark spectra would be sufficient for detection (the number of components observed depends strongly on the field intensity) but would not have any field-induced broadening.

We can work from this spectrum to find the scalar and tensor polarizabilities of the $36P$ and $37P$ levels. The frequency interval between the two outermost low-frequency components (which correspond to the transitions $36P_{3/2,3/2} \to 37P_{3/2,1/2}$ and $36P_{3/2,1/2} \to 37P_{1/2,1/2}$) determines the tensor polarizability of the $36P_{3/2}$ level. When the measurement error is taken into account [this error stems from the error in the measurements of the frequency differences (1 MHz) and the error in the measurements of the
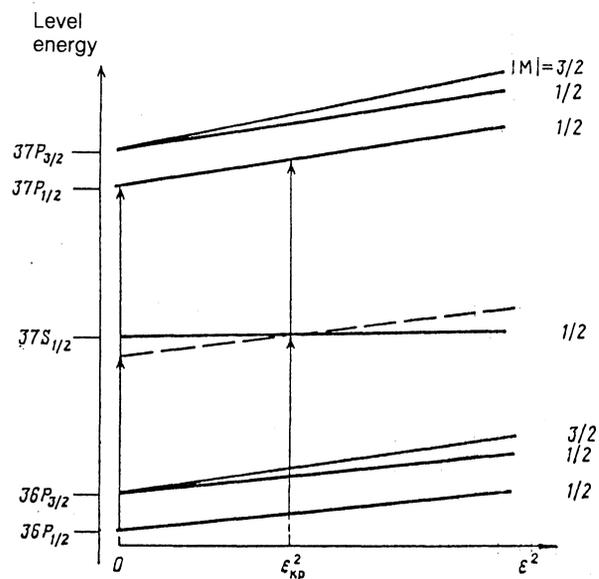


FIG. 6. Splitting of Rydberg levels of Na in a static electric field in the model of the quadratic Stark effect, along with a physical picture of the appearance of a double Stark resonance on the $nP \to (n+1)P$ transitions. a—$E = 0$; b—2.2 V/cm.
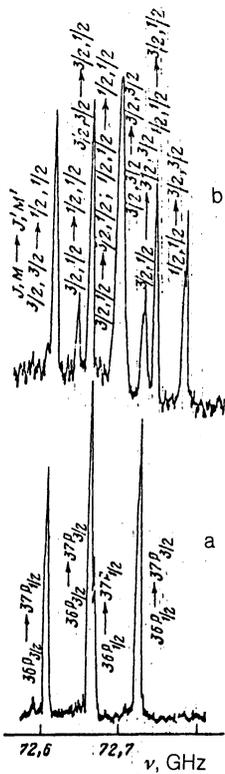
FIG. 7. Experimental observation of the influence of the static Stark effect on the spectrum of the two-photon transition $36P$–$37P$ in the Na atom. a—$E = 0$; b—2.2 V/cm. The microwave intensity is $I \approx 10^{-7}$ W/cm$^2$.

field ($\sim0.1$ V/cm)], we find $\alpha_2(36P_{3/2}) = (12.4 \pm 1.5)$ MHz/(V/cm)$^2$. Correspondingly, the two outermost high-frequency components (corresponding to the transition $36P_{1/2,1/2} \rightarrow 37P_{3/2,1/2}$ and $36P_{1/2,1/2} \rightarrow 37P_{3/2,3/2}$) yield the value $\alpha_2(37P_{3/2}) = (16.3 \pm 2)$ MHz/(V/cm)$^2$. Determining the scalar polarizabilities is a slightly more complicated process, since the intermediate components in the spectrum cannot be identified unless we know the values of $\alpha_0(36P)$ and $\alpha_0(37P)$, and from the four components which we mentioned we can find only differences between scalar polarizabilities. Preliminary analysis of the spectrum showed that a correct description would require that $\alpha(36P_{1/2})$ and

$\alpha_0(36P_{3/2})$ be assumed to be different, although not by much [the polarizabilities with the same $J$'s and different $n$'s should be related to each other by (13)]:

$$\alpha_0(37P_{1/2}) = \alpha_0(36P_{1/2}) \frac{[37 - \delta(37P_{1/2})]^7}{[36 - \delta(36P_{1/2})]^7}, \quad (14)$$

$$\alpha_0(37P_{3/2}) = \alpha_0(36P_{3/2}) \frac{[37 - \delta(37P_{3/2})]^7}{[36 - \delta(36P_{3/2})]^7}, \quad (15)$$

where $\delta(nJ)$ is the quantum defect of level $P$ in the Na atom, which is given by (6).

We can thus determine the following quantities from the spectrum in Fig. 7b:

$$\alpha_0(36P_{1/2}) - \alpha_0(37P_{1/2}) = (18\pm3) \text{ MHz/(V/cm)}^2, \quad (16)$$

$$\alpha_0(36P_{3/2}) - \alpha_0(37P_{3/2}) = (30\pm5) \text{ MHz/(V/cm)}^2, \quad (17)$$

Using (14) and (15), we find a closed system of equations, so we can calculate the changes in the scalar polarizabilities for the $36P$ and $37P$ levels. The results of all the measurements are shown in Table I. Also shown there are values of the polarizabilities calculated from the theoretical results of Ref. 23 (including results on the $37S$ level). Those calculations were carried out through the use of the dipole matrix elements found in the WKB-MKD approximation. Comparison with our experimental data shows that the theory predicts polarizability values which are slightly smaller. The reason may be the error in the approximation of the energy levels in Na on the basis of the quantum defect. Further support for the validity of our measurements comes from the close agreement of these results with the results of measurements of the polarizabilities of $P$ levels in Ref. 24 [data for the $34P$ and $41P$ levels were given in that study; those results can be used to calculate polarizabilities of the $36P$ and $37P$ levels with the help of Eq. (13)].

A distinctive feature of our calculations is the observation of the difference between the scalar polarizabilities of levels for different fine-structure components. It has previously been assumed that these polarizabilities are the same. The differences between the scalar polarizabilities for the $J = 1/2$ and $J = 3/2$ components of the $36P$ and $37P$ levels are

$$\alpha_0(36P_{1/2}) - \alpha_0(36P_{3/2}) = (5\pm1) \text{ MHz/(V/cm)}^2,$$

$$\alpha_0(37P_{1/2}) - \alpha_0(37P_{3/2}) = (7\pm2) \text{ MHz/(V/cm)}^2.$$

TABLE I. Experimental and theoretical values of the polarizabilities of the $36P$, $37P$, and $37S$ levels of the Na atom, in units of MHz/(V/cm)$^2$.

| Level | Theory[22] | | Experimental[23]* | | Experimental (present study) | |
|-------|------------|------------|------------|------------|------------|------------|
| | $\alpha_0$ | $\alpha_2$ | $\alpha_0$ | $\alpha_2$ | $\alpha_0$ | $\alpha_2$ |
| $37S_{1/2}$ | +6,2 | 0 | – | – | – | – |
| $36P_{1/2}$ | –91,6 | 0 | –113,6 | 0 | –105±10 | 0 |
| $36P_{3/2}$ | –91,6 | –9,2 | –113,6 | –12,4 | –110±11 | –12,4±1,5 |
| $37P_{1/2}$ | –112,0 | 0 | –138,3 | 0 | –128±13 | 0 |
| $37P_{3/2}$ | –112,0 | –11,2 | –138,3 | –15,0 | –135±13 | –16,3±2 |

*The polarizabilities of the $36P$ and $37P$ levels were found by approximating the polarizabilities measured in Ref. 23 for the $34P$ and $41P$ states by an $(n_{\text{eff}})^7$ law.

The errors in the measurements of these differences are far smaller than the errors in the determination of the absolute values of these polarizabilities.

Further support for the validity of these measurements comes from the fact that the positions of the other components in Fig. 7b are described quite accurately by expression (12) if we use the values found for the scalar and tensor polarizabilities. The strong central line contains three unresolved components with approximately equal frequencies in this case. This circumstance explains why the spectrum has seven instead of nine components. All the components have been identified as $36P_{J,|M|} \rightarrow 37P_{J'|M'|}$ transitions.

The relative intensities of the components are determined by the two-photon matrix elements for each transition, by the polarization of the microwave field with respect to the static field E, and by the population of the Stark sublevels of the 36P level. The latter depends on the spectral power and the polarization of the light of the third-step laser, in resonance with the $4S \rightarrow 36P$ transition. It is a rather complicated matter to determine the polarization of microwave radiation directly. The polarization vector of the wave probably has both a z component and a component in the plane perpendicular to the z axis, since the spectrum has both transitions with $\Delta M = 0$, induced by the z component of the polarization vector, and transitions with $\Delta M = \pm 1$, induced by a component in the XY plane.

In stronger electric fields, the Stark spectrum of the two-photon transition $36P \rightarrow 37P$ changes dramatically. Figure 8 shows spectra recorded as the electric field was varied
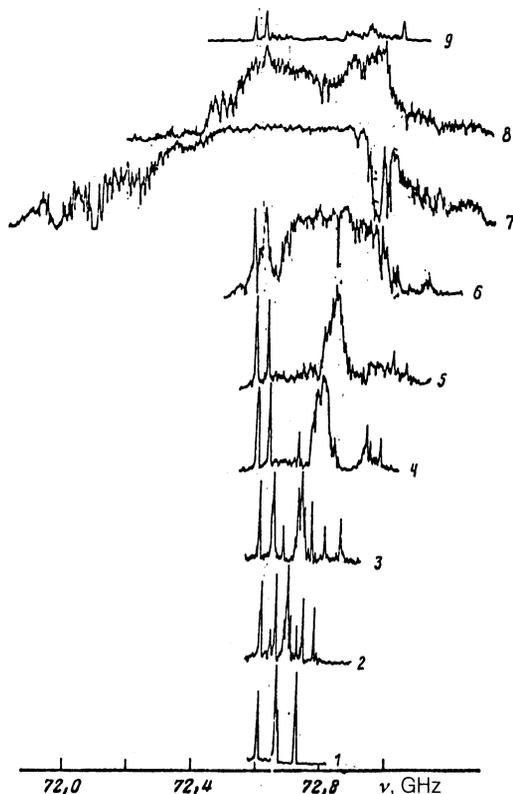


FIG. 8. Appearance of the double Stark resonance on the two-photon transition 36P–37P with increasing strength of the static electric field. 1—0 V/cm; 2—2.2; 3—3.3; 4—4.4; 5—5.0; 6—5.5; 7—6.1; 8—6.6; 9—7.2 V/cm.

from 0 to 7 V/cm, at a fixed microwave power. A characteristic effect here is the appearance of a broad, weakly resonant band (with a width of about 1 GHz) near 6 V/cm. This band is seen in a rather narrow interval of electric fields (between 5.5 and 6.6 V/cm). This interval depends on the intensity. Some of the two-photon peaks remain resonant, while others are completely lost in this spectrum. A further increase in the electric field restores the usual Stark picture of the spectrum of two-photon transitions.

The physical nature of the broad band in the spectrum of two-photon absorption at fields near 6 V/cm can be understood on the basis of the Stark diagram of the levels (Fig. 6) constructed in accordance with the values found for the polarizabilities (Table I). For the 37S level we used a polarizability calculated from the data of Ref. 23.

The signs of the polarizabilities of these levels are such that the imposition of an external electric field reduces the deviation of the real intermediate 37S level from the virtual level of the two-photon transition. At some value $E_{cr}$ of the electric field these levels cross, and the two-photon resonance becomes a double resonance. As a result, there is a sharp increase in the probability for the 36P transition and a field-induced broadening of this transition. The values of $E_{cr}$ are different for the different components of the fine structure of the 36P and 37P levels between which the transition occurs. As a result, some of the two-photon resonances remain in the spectrum, while those which have reached the exact double resonance undergo a pronounced field-induced broadening.

It is difficult to find a theoretical estimate of the width of the band in this case, since a large number of levels may become involved in the interaction. The reason is that the system is not, strictly speaking, a three-level system. Nevertheless, we can estimate the width of the observed double resonance in the approximation of a three-level scheme for the case in which the dipole moments of transitions from P levels to an intermediate S level are the same. In this case, by analogy with Ref. 19, the system of equations reduces to the cubic equation

$$\mu^3 + 3\Omega\mu^2 + 2[\Omega^2 - \gamma^2]\mu - 2\gamma^2\Omega = 0, \tag{18}$$

where $\gamma = (D_z\varepsilon)/2\hbar$ is the one-photon Rabi frequency, and $\Omega$ is the frequency difference. The roots of this equation can be found easily. It thus becomes possible to find the time evolution of the population of the upper level of the double resonance and the field-induced broadening of the transition:

$$\rho_2 = |a_2|^2 = \left[\frac{\gamma^2}{(\Omega^2/4)^2 + \gamma^2}\right]^2 \sin^4 \frac{(2\gamma^2 + \Omega^2)^{1/2}}{2} t. \tag{19}$$

The first factor here describes the width of the resonance, which is given approximately by

$$\Delta v \approx D_z\varepsilon/10\hbar, \tag{20}$$

where $D_z$ is the dipole moment of the $36P \rightarrow 37S$ transition, and $\varepsilon$ is the microwave field. For the transition $36P_{3/2} \rightarrow 37S_{1/2} \rightarrow 37P_{1/2}$ expression (20) yields a field-induced broadening of 0.3 GHz at a microwave power $\sim 10^{-4}$ W/cm$^2$. This figure is close in order to magnitude to the observed width of the double resonance.

Another distinguishing feature of the spectrum in Fig. 8 is that its components behave identically as functions of $E$. The extreme low-frequency component (corresponding to the transition $36P_{3/2,3/2} \rightarrow 37P_{1/2,1/2}$) shifts up the frequency scale in weak fields, $< 3$ V/cm. In other words, the polarizability of the $37P_{1/2,1/2}$ level is greater than that of the $36P_{3/2,3/2}$ level. However, the shift of this component subsequently deceases and even changes sign, with the result that this component begins to move toward lower frequencies. We can thus say that we are observing an "anticrossing" of levels,[22] which results from an interaction of $36P$ and $37P$ states with the Stark series corresponding to higher angular momenta $l > 2$. In fields $> 5$ V/cm, the component at the far right in the spectrum (corresponding to the transition $36P_{1/2,1/2} \rightarrow 37P_{3/2,3/2}$) begins to shift sightly more rapidly than according to (12) (Fig. 9). The meaning here is that the Stark effect in the $36P$ and $37P$ levels generally ceases to be quadratic at fields as weak as $> 5$ V/cm, and expression (12) can describe the shifts only within a certain error.

The observation of shifts and splittings of the spectral components of two-photon $P \rightarrow P$ transitions has made it possible to determine the range of applicability of the quadratic-effect approximation and to measure the scalar and tensor polarizabilities of the $P$ levels. The experimental data turn out to lie close to the calculated results. The appearance of the double Stark resonance on the two-photon $P \rightarrow P$ transition of the electric field can be classified as a new effect. There is the possibility that this effect might be utilized for an absolute calibration of weak electric fields in vacuum.[25]

## 5. ABSOLUTE CALIBRATION OF ELECTRIC FIELDS THROUGH STARK FINE-TUNING OF A DOUBLE MICROWAVE RESONANCE

The critical electric field for the occurrence of a double Stark resonance depends on the particular transition between Stark components, $36P_{J|M|} \rightarrow 37P_{J'|M'|}$. In the quadratic-Stark-effect approximation this field is given by

$$E_{cr}^2 = \frac{2\nu(37S_{1/2}) - \nu(37P_{J'}) - \nu(36P_J)}{\alpha(37S_{1/2}) - 0,5\alpha(37P_{J'|M'|}) - 0,5\alpha(36P_{J|M|})},$$

$$(21)$$

where $\nu\Delta(37S_{1/2})$, $\nu(36P_{J'})$, and $\nu(36P_J)$ are the corresponding unperturbed energy levels, in frequency units, and the $\alpha$'s are the total polarizabilities of these sublevels. Table II shows values of $E_{cr}$ calculated from (21), along with the corresponding frequencies which would be expected for double microwave resonances. The range of $E_{cr}$ (from 5.9 to 6.6 V/cm) corresponds to electric fields in which the double Stark resonance is observed on the two-photon transition $36P \rightarrow 37P$.

The electric field scale can be found in the following way. The frequency of the microwave field is fixed near one of the values in Table II. The electric field strength is swept, and the population of the $37P$ level is measured. When $E_{cr}$ is reached, a resonance corresponding to $E_{cr}$ should appear in the spectrum recorded in this manner. The position of this resonance determines the electric field scale; the accuracy of the calibration is determined by the width, which in turn depends on the microwave power. This power should be chosen at a level such that a sufficient signal-to-noise ratio is achieved with minimum field-induced broadening of the
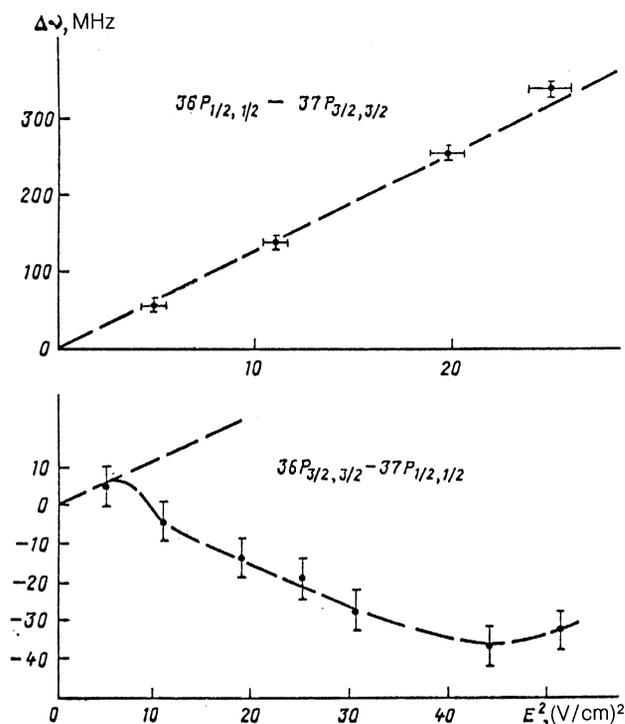


FIG. 9. Frequency shift of the outermost components of the Stark spectrum of the two-photon $36P \rightarrow 37P$ transition versus the electric field.

peak. However, the probability for the $36P \rightarrow 37S \rightarrow 37P$ double resonance is so high that field-induced broadening is observed even at the lowest microwave power. On the other hand, this circumstance simplifies the fine tuning of the frequency, which is a rather complicated problem in the case of narrow peaks.

Experimental spectra of this type were recorded for various values of the power and frequency of the microwave radiation. As before, the intensity was calibrated on the basis of the field-induced broadening of the $36P_{1/2} \rightarrow 37P_{3/2}$ transition in the absence of an electric field. Figure 10 shows spectra recorded by sweeping the electric field at a microwave frequency of 72.9 GHz. Here we see a narrow peak at 5.9 V/cm, which corresponds, according to Table II to the $36P_{3/2,3/2} \rightarrow 37P_{3/2,3/2}$ transition, which has the lowest critical field. This result is evidence of a high probability for the double resonance $36P_{3/2,3/2} \rightarrow 37S_{1/2,1/2} \rightarrow 37P_{3/2,3/2}$. Consequently, it is not necessary to fine-tune the frequency of the microwave field to this transition exactly. The width of the $36P_{3/2,3/2} \rightarrow 37P_{3/2,3/2}$ resonance is about 0.1 V/cm at a power $\sim 4 \cdot 10^{-7}$ W/cm$^2$. This quantity determines the accuracy of the calibration of the electric field in our experiments. At a certain microwave intensity, we also find a peak near 6.6 V/cm in the spectrum. This peak can be attributed to the four transitions in Table I, so this peak is rather difficult to identify, in view of the errors in the measurements of the frequency and the electric field. Nevertheless, the presence of this peak confirms that it is legitimate to use expression (2) to determine $E_{cr}$ for the various transitions.

An increase in the microwave intensity not only gives rise to signals at fields 6.0–7.0 V/cm, which correspond to

TABLE II. Critical fields and frequencies for an absolute calibration of the electric field through a Stark fine-tuning of a double microwave resonance (a double Stark resonance).

| Transition | $\alpha\ (36P_{J\,\|M\|})$, MHz/(V/cm)$^2$ | $\alpha\ (37P_{J'\|M'\|})$, MHz/(V/cm)$^2$ | $2E_{cr}$, V/cm | $\nu_{cr}$, GHz |
|---|---|---|---|---|
| $36P_{3/2,\,3/2} \rightarrow 37P_{1/2,\,1/2}$ | $-122,5$ | $-128,25$ | 6,23 | 72,662 |
| $36P_{3/2,\,3/2} \rightarrow 37P_{3/2,\,1/2}$ | $-122,5$ | $-118,5$ | 6,28 | 72,631 |
| $36P_{3/2,\,3/2} \rightarrow 37P_{3/2,\,3/2}$ | $-122,5$ | $-151,4$ | 5,91 | 72,918 |
| $36P_{3/2,\,1/2} \rightarrow 37P_{1/2,\,1/2}$ | $-97,7$ | $-128,25$ | 6,53 | 72,919 |
| $36P_{3/2,\,1/2} \rightarrow 37P_{3/2,\,1/2}$ | $-97,7$ | $-118,5$ | 6,61 | 72,897 |
| $36P_{3/2,\,1/2} \rightarrow 37P_{3/2,\,3/2}$ | $-97,7$ | $-151,4$ | 6,18 | 73,176 |
| $36P_{1/2,\,1/2} \rightarrow 37P_{1/2,\,1/2}$ | $-105,4$ | $-128,25$ | 6,52 | 72,910 |
| $36P_{1/2,\,1/2} \rightarrow 37P_{3/2,\,1/2}$ | $-105,4$ | $-118,5$ | 6,58 | 72,872 |
| $36P_{1/2,\,1/2} \rightarrow 37P_{3/2,\,3/2}$ | $-105,4$ | $-151,4$ | 6,17 | 73,166 |

Table II, but also gives rise to signals at fields far below the calculated values. These are probably signals representing Stark fine-tuning of multiphoton resonances of higher order.[26] At any rate, the calibration of a static electric field should be carried out at microwave intensities such that this effect has not yet appeared.

We conclude with a few words about the accuracy of an absolute calibration of the electric field by the method of Stark tuning of the double microwave resonance. The accuracy of 0.1 V/cm is not a limit. The error in measurements of $E_{cr}$ is determined by the width of the source line. According to (21), it is

$$\Delta E \sim \frac{2\Delta\nu}{E_{cr}\,[\alpha(37S_{1/2}) - \tfrac{1}{2}\alpha(37P_{J'\|M'\|}) - \tfrac{1}{2}\alpha(36P_{J\|M\|})]},$$
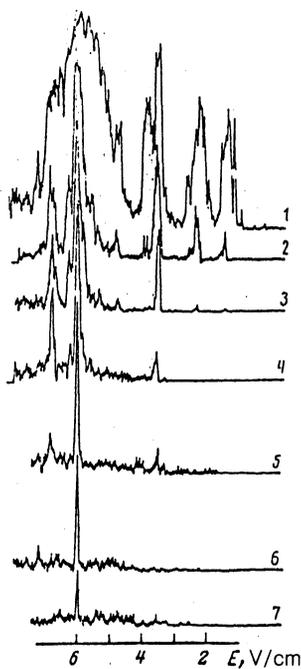
(22)



FIG. 10. Experimental spectrum of the double Stark resonance recorded as the electric field was swept at a fixed microwave frequency, 72.9 GHz. *1*—The microwave intensity is $8\cdot10^{-6}$ W/cm$^2$; *2*—$4\cdot10^{-6}$; *3*—$2\cdot10^{-6}$; *4*—$8\cdot10^{-7}$; *5*—$4\cdot10^{-7}$; *6*—$8\cdot10^{-8}$; *7*—$4\cdot10^{-8}$ W/cm$^2$.

where $\Delta\nu$ is the width of the source line. In the absence of field-induced broadening, we find $\Delta E \sim 10^{-2}$ V/cm for the $36P_{3/2,3/2} \rightarrow 37P_{3/2,3/2}$ transition from this expression with $\Delta\nu \sim 2$ MHz (a typical figure for our experiments). If a microwave source with a narrower line is used, $\Delta\nu$ will be determined by the transit-time broadening in the detection system, which is $\sim 0.2$ MHz. In this case the accuracy of the calibration reaches $10^{-3}$ V/cm. The use of "cold" Rydberg atoms makes it possible to achieve a further improvement in the accuracy of measurements of electric fields in vacuum, by the method of Stark fine-tuning of the double microwave resonance. Such accuracies are extremely difficult to achieve by any other methods for measuring electric fields.

By observing the double resonance at other $nP \rightarrow (n+1)P$ transitions, in both the Na atom and other alkali metal atoms (Cs, Rb, Li, K) one can compile a set of reference points for determining the electric field, since $E_{cr}$ depends on both $n$ and the particular chemical element. The higher the excitation level, the weaker the field $E_{cr}$ required for this purpose, since the polarizability increases as $(n_{eff})$.[7] To demonstrate this idea, we carried out some experiments on the microwave spectroscopy of the $37P \rightarrow 38P$ two-photon transition. Figure 4b shows the spectrum of this transition in the absence of a static external electric field. The frequency positions of the peaks are close to the values calculated from the data of Ref. 18, but there is a deviation of 5 MHz in the positions of the resonances corresponding to the transitions $37P_{3/2} \rightarrow 38P_{3/2}$ and $37P_{1/2} \rightarrow 38P_{1/2}$. This deviation goes beyond the measurement error. It is quite possible that for $P$ levels with $n > 37$ there are deviations from the $(n_{eff})^{-3}$ law for the fine-structure intervals.

Figure 11 shows a Stark spectrum of the $37P \rightarrow 38P$ two-photon transition at a microwave intensity lower than that in Fig. 4b. As for the $36P \rightarrow 37P$ transition, we find a splitting due to the quadratic Stark effect in weak fields. With increasing field, we see the appearance of a double Stark resonance near 5.5 V/cm. The calculated value is $E_{cr} = 5.5$ V/cm for the $37P_{3/2,3/2} \rightarrow 38P_{3/2,3/2}$ transition in the region in which the band appears. An anomalous result in this case is the frequency position of the broadened double-resonance band. This band is shifted into the low-frequency part of the spectrum, in which there should be no signals at all according to calculations based on the quadratic Stark effect. At the same time, the components at higher frequencies disappear. To study the shift of the band into the low-frequency part of the
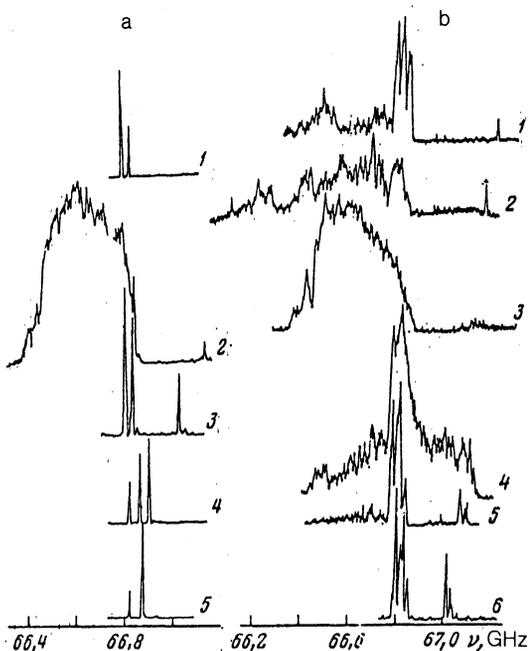
FIG. 11. Appearance of a double Stark resonance on the $37P \to 38P$ two-photon transition. a: Total Stark spectrum of the transition. $1$—$E = 6.6$ V/cm; $2$—5.5; $3$—4.4; $4$—2.2; $5$—0 V/cm. b: Frequency shift of the double resonance at low frequencies. $1$—$E = 6.08$ V/cm; $2$—5.81; $3$—5.53; $4$—5.25; $5$—5.00; $6$—4.42 V/cm.

spectrum in more detail, we recorded the Stark spectrum of the $37P \to 38P$ transition, at a smaller step in the electric field. These results confirmed the anomalies. These anomalies are probably due to a "repulsion" of either $nP$ or $nS$ states due to a crossing with the Stark sequence for states with higher angular momenta. As a result, the approximation of a quadratic Stark effect becomes incorrect, and it is no longer possible to calculate the critical frequencies and fields from simple formulas. Nevertheless, there is the important result that the double Stark resonance can be observed at various values of $E_{cr}$ and on other two-photon transitions. It is thus possible to compile a set of reference points for an absolute calibration of electric fields in vacuum.

## 6. CONCLUSION

In these experiments, we studied the basic aspects of microwave spectroscopy of two-photon absorption on $P$–$P$ transitions of Rydberg states of the Na atom. We studied the Stark effect in static electric fields, determined the range of applicability of the quadratic effect, and found values for the scalar and tensor polarizabilities of the $nP$ states. We have observed that avoided crossings influence the Stark spectra of the two-photon absorption. We have experimentally observed the crossing of a real level and a virtual level of $nP \to (n + 1)P$ two-photon transitions in Rydberg atoms. We have also observed the appearance of a double Stark resonance. We have recorded spectra of the double Stark resonance along the electric field scale, and we have discussed the possibility of using this resonance for an absolute calibration of electric fields in vacuum. The experimental data reported here will be of assistance in reaching a deeper understanding of the resonant and quasiresonant interactions of highly excited (Rydberg) atoms with microwave radiation in future research. In particular, this information is important for describing the physical picture of the formation of a quasicontinuum during the joint occurrence of the dynamic and static Stark effects. In this case, the microwave intensity required for ionizing Rydberg atoms is sharply reduced.[27]

[1] B. W. Shore, *The Theory of Coherent Atomic Excitation*, Wiley, New York, 1990.

[2] W. Demtroder, *Laser Spectroscopy*, Springer-Verlag, New York, 1981 (Russ. Transl., ed. I. I. Sobel'man), Nauka, Moscow, 1985).

[3] K. Shimoda, in *Laser Spectroscopy of Atoms and Molecules* (ed. H. Walther), Springer-Verlag, New York, 1976 (Russ. Transl. Mir, Moscow, 1979).

[4] K. Shimoda and T. Shimizu, *Nonlinear Spectroscopy of Molecules* (Prog. Quant. Elect., Vol. 2, Part 2), Pergamon, Oxford, 1972.

[5] V. S. Letokhov and V. P. Chebotaev, *Nonlinear Ultrahigh-Resolution Laser Spectroscopy*, Nauka FM, Moscow, 1990.

[6] I. M. Beterov and V. P. Chebotaev, *Three-Level Gas Systems and Their Interaction with Radiation* (Prog. Quant. Elect., Vol. 3, Part 1), Pergamon, Oxford, 1974.

[7] I. M. Beterov, Yu. A. Matyugin, and V. P. Chebotaev, Zh. Eksp. Teor. Fiz. **64**, 1495 (1973) [Sov. Phys. JETP **37**, 756 (1973)].

[8] N. B. Delone and V. P. Krainov, *Atoms in Strong Light Fields (Springer Series in Chemical Physics: Vol. 28)*, Energoatomizdat, Moscow, 1984 (Springer-Verlag, New York, 1985).

[9] S. G. Rautian, *Invited Paper, Second Conference on Multiphoton Processes*, CRIP, Budapest, 1975, p. 150.

[10] P. F. Liao and J. E. Bjorkholm, Phys. Rev. Lett. **34**, 1540 (1975).

[11] I. M. Beterov, G. L. Vasilenko, B. M. Smirnov, and N. V. Fateev, Zh. Eksp. Teor. Fiz. **93**, 31 (1987) [Sov. Phys. JETP **66**, 17 (1987)].

[12] I. M. Beterov, G. L. Vasilenko, I. I. Riabtzev et al., Z. Phys. D **6**, 55 (1987).

[13] B. M. Smirnov, *Excited Atoms*, Energoatomizdat, Moscow, 1982.

[14] R. A. Ambartsumyan, G. I. Bekov, V. S. Letokhov, and V. I. Mishin, Pis'ma Zh. Eksp. Teor. Fiz. **21**, 595 (1975) [JETP Lett. **21**, 279 (1975)].

[15] M. B. Kadomtsev and B. M. Smirnov, Zh. Eksp. Teor. Fiz. **80**, 1715 (1981) [Sov. Phys. JETP **53**, 885 (1981)].

[16] I. M. Beterov, I. I. Ryabtsev, and N. V. Fateev, Pis'ma Zh. Tekh. Fiz. **15**, 40 (1989) [Sov. Tech. Phys. Lett. **15**(6), 430 (1989)].

[17] I. M. Beterov, I. I. Ryabtsev, and N. V. Fateev, Pis'ma Zh. Eksp. Teor. Fiz. **48**, 181 (1988) [Sov. Phys. JETP **48**, 195 (1988)].

[18] C. Fabre, S. Haroche, and P. Goy, Phys. Rev. A **22**, 778 (1980).

[19] V. S. Letokhov, *Laser Photoionization Spectroscopy*, Nauka FM, Moscow, 1987.

[20] C. Fabre and S. Haroche, *Spectroscopy of One- and Two-Electron Atoms (Rydberg States of Atoms and Molecules)* (Russ. Transl. Mir, Moscow, 1985).

[21] S. P. Goreslavskiĭ, N. B. Delone, and V. P. Kraĭnov, Zh. Eksp. Teor. Fiz. **82**, 1789 (1982) [Sov. Phys. JETP **55**, 1032 (1982)].

[22] I. I. Sobel'man, *Introduction to the Theory of Atomic Spectra*, Pergamon, Oxford, 1972.

[23] V. A. Davydkin and B. A Zon, Opt. Spectrosc. **52**, 600 (1982) [Opt. Spectrosc. (USSR) **52**, 359 (1982)].

[24] C. Fabre, S. Haroche, and P. Goy, Phys. Rev. A **18**, 229 (1978).

[25] I. M. Beterov, G. L. Vasilenko, V. P. Kraĭonov et al., Pis'ma Zh. Tekh. Fiz. **17**, No. 9, 44 (1991) [Sov. Tech. Phys. Lett. **17**, 331 (1991)].

[26] I. M. Beterov and N. V. Fateev, Izv. Akad. Nauk SSSR, Ser. Fiz. **53**, 1457 (1989).

[27] P. Pillet, C. H. Mahon, and T. F. Gallagher, Phys. Rev. Lett. **60**, 21 (1988).